

Theoretical Conformational Analysis of Thiacycrown Macrocycles

Susan E. Hill and David Feller*

Environmental Molecular Sciences Laboratory, Pacific Northwest National Laboratory, MS K8-91,
P.O. Box 999, Richland, Washington 99352

Received: September 9, 1999; In Final Form: November 8, 1999

A gas phase conformational analysis was performed on four sulfur-containing macrocycles (9-thiacycrown-3, 12-thiacycrown-4, 15-thiacycrown-5, and 18-thiacycrown-6) using a combination of empirical and ab initio methods. Candidates for low-lying conformers were initially generated from high-temperature molecular dynamics simulations. A more computationally manageable subset of conformations was selected for further study based on their relative energies at successively higher levels of ab initio theory. The highest level of theory included second-order perturbation theory with the aug-cc-pVDZ basis set. The lowest conformation of 9-thiacycrown-3 was found to have an exodentate C_2 structure with an electronic energy that is 4 kcal/mol below the C_3 crystal structure. For 12-thiacycrown-4, the lowest energy structure possesses D_4 structure in both the gas and crystal phase. In the case of 15-thiacycrown-5 the lowest energy conformer possesses an oblong, partially exodentate, gas phase structure with C_2 symmetry. The crystal structure has C_1 symmetry and lies 3 kcal/mol higher in energy. 18-Thiacycrown-6 has an exodentate C_2 symmetry, which is estimated with a large uncertainty to be 1 kcal/mol below the folded C_2 structure of the crystal. Zero-point vibrational effects shift relative energies by up to 0.3 kcal/mol across an energy span of 5–7 kcal/mol, but the effect on close-lying conformers is less.

I. Introduction

Interest in oxygen-bearing crown ethers stems from their remarkable ability to selectively bind specific cations in complex solutions contaminated with chemically similar cations. Most of the theoretical work in this area has focused on isolated 18-crown-6 (18c6) in the gas phase,^{1–3} in solution,^{4–8} and in complexes formed with metal cations.^{9–22} Comparatively little effort has gone into understanding the sulfur-bearing analogues of crown ethers known as thiacycrowns. Unlike oxygen-bearing crowns, which tend to preferentially bind main group metal cations, thiacycrowns prefer transition metal cations.²³

Another difference between oxygen-bearing and sulfur-bearing crown can be found in their conformational preferences. The former prefer “endodentate” conformations in which the oxygens are oriented toward the center of the macrocycle cavity. The resulting region of negative electrostatic potential that lines the inside of the cavity creates an ideal receptacle for a cation. Oxygen-bearing crowns are said to be “preorganized” for cation binding. This preference for endodentate conformations requires an underlying preference for gauche dihedral angles about C–C bonds and trans angles about C–O bonds.

Thiacycrowns prefer “exodentate” structures in which the sulfur atoms are pointing away from the cavity interior, creating a lining of hydrogen atoms. This difference with oxygen-bearing crowns is principally due to the longer carbon–electron donor atom distances (1.8 Å C–S vs 1.4 Å C–O). The longer bond lengths result in negligible 1,4 repulsions between terminal hydrogens, allowing the CCSC subunit to assume a gauche torsional angle. The S···S interactions are slightly repulsive (repulsive gauche effect), which leads to a trans torsion about the C–C bond. Consequently, in order for thiacycrowns to bond

with a metal cation, it is necessary to first distort the crown macrocycle to permit multiple metal–sulfur bonds, a step which bears an energetic cost.^{24,25} Rather than pay this penalty, thiacycrowns can encompass a cation by forming bridged and/or sandwich complexes.^{26–30}

We have previously studied the oxygen-bearing crowns known as 12-crown-4,^{20,31} 15-crown-5,³² and 18-crown-6.³³ In this paper, we turn our attention to a conformational analysis of 9-thiacycrown-3 (1,4,7-trithiacyclononane), 12-thiacycrown-4 (1,4,7,10-tetrithiacyclododecane), 15-thiacycrown-5 (1,4,7,10,13-pentathiacyclopentadecane), and 18-thiacycrown-6 (1,4,7,10,13,16-hexathiacyclooctadecane), crowns in which sulfur has completely replaced oxygen as the electron donor. Hereafter, we will refer to these molecules as 9t3, 12t4, 15t5, and 18t6, respectively. Our approach relies on a combination of molecular mechanics and ab initio quantum mechanical methods. Reliable information about the low-lying conformations of thiacycrowns is important for subsequent ab initio studies of the binding preferences of thiacycrowns for metal cations and as a check on the accuracy of less sophisticated theoretical models. Previous studies comparing ab initio conformational energy orderings with those predicted by the MM3 force field³⁴ and AM1 or PM3 semiempirical methods³⁵ reported that the results were sensitive to the level of theory used. As will be shown, crystal structures are not a reliable indicator of the lowest lying conformations in the gas phase.

We will also explore the torsional potential energy surfaces of 1,2-dimethoxyethane (DXE = CH₃OC₂H₄OCH₃) and 1,2-dimethylthioethane (DTE = CH₃SC₂H₄SCH₃) as models of (–OC₂H₄O–)_n and (–SC₂H₄S–)_n linkages in the large ring limit. Although the global minimum is the natural reference state for computing M⁺–thiacycrown binding energies, if there are many low-lying conformers, experimental techniques, such as

* To whom correspondence should be addressed.

collision-induced dissociation, will measure the dissociation with respect to a Boltzmann distribution of states.^{36–41} This assumes that the barriers to interconversion of one conformation to another are small. While a comprehensive study of such barriers is beyond the scope of the present work, due to computational difficulty of locating transition states in large, flexible molecules, lower bounds can be estimated on the basis of the barriers in DXE and DTE.

II. Modeling Strategy

The search for low-lying conformers in floppy molecules is hindered by the sheer number of local minima on the potential surface and the lack of rigorous mathematical tools to guarantee that a global minimum has been identified.^{42,43} Algorithms for conformational searching typically use molecular dynamics (MD), systematic (i.e., grid-based) or stochastic (i.e., Monte Carlo based) search techniques.^{44–47} Böhm et al.⁴⁸ compared five algorithms on a nine-membered lactam and concluded that most of the methods sampled roughly equivalent portions of configuration space, but the energy ordering of the conformers was strongly dependent upon the details of the theoretical treatment. In order to characterize a stationary point as a minimum, it is necessary to examine the spectrum of normal-mode frequencies, a step which was not done in the study of Böhm et al.⁴⁸ Previous conformational studies that included normal-mode analyses and spanned empirical, semiempirical, and ab initio theoretical approaches also emphasized the sensitivity of the conclusions to the level of theory.^{42,49}

The adoption of low-level geometries for subsequent higher level energy evaluations (without reoptimization) is a widespread practice that, when properly calibrated, can provide significant savings in computer time with little loss in accuracy.⁴⁹ However, if the gap between the levels of theory is too great, reliance on low-level geometries can introduce a degree of uncertainty sufficient to outweigh the potential improvement to be gained from the higher-level energy calculations. Reoptimization at an intermediate level of theory can serve to minimize such difficulties. In the present work, abrupt changes in the level of theory (e.g., large basis set MP2 energy evaluation at geometries obtained from force field optimizations) were avoided. It should be noted that no approach short of optimizing each candidate structure at the highest level of theory, followed by normal-mode analyses to guarantee that the stationary points are true minima, is without problems. For example, a recent study of the rotational conformations of α,α' -diaminoacetone demonstrated that minima identified at the HF/6-31+G* level were missed with smaller basis sets.⁵⁰ Unfortunately, examining every potential structure identified by molecular mechanics at the highest level of theory is not currently feasible for the thiacycrows examined in this study. Since most optimization algorithms in common use provide no guarantee that the stationary points they locate are minima, a normal-mode analysis is a necessary step and increases the cost of the search significantly.

Our strategy involves (1) the use of high-temperature MD simulations to sample a large volume of configuration space and generate a (potentially large) number of candidate conformers, (2) subsequent MM optimization of the structures to reduce the number of candidates for ab initio optimization to fewer than 20, and (3) further optimization and normal-mode analysis of all conformations below some predefined energy threshold using small-to-intermediate sized basis set RHF calculations and (4) single-point MP2 energies. For a limited number of cases, larger basis set MP2 geometry optimization was performed. Details of the approach are given below.

Crystal structures for the four thiacycrows were taken from the Cambridge Structural Database (CSD)⁵¹ and subjected to RHF/6-31+G* geometry optimization^{52–54} using Gaussian 94.⁵⁵ The diffuse functions present in the 6-31+G* basis set were removed from carbon and hydrogen, since our previous work on oxygen-bearing ethers showed them to be unimportant for computing geometries and binding energies. Atomic partial charges were obtained from the CHELPG algorithm⁵⁶ and were modified so as to represent average values for a neutral CH₃-SCH₃ polymer unit, the magnitudes of which show a slight dependence on ring size. Although the charges on sulfur were essentially constant across the four compounds, carbon and hydrogen charges varied by a factor of 3. For example, the charge on carbon varied from a low of 0.13 e⁻ in 12t4 to a high of 0.41 e⁻ in 9t3. The partial charges were combined with the standard consistent valence force field (CVFF)⁵⁷ in order to perform MD simulations. The thiacycrows were equilibrated at 2000 K in five steps of 0.2 ps each. High temperatures were required in order to drive the thiacycrows over conformational barriers and achieve exo \rightarrow endodontate changes. MD simulations and MM minimizations were done using the code Argus 3.0.^{58,59}

MD simulations were then run with a time step of 0.5 fs for a total runtime of 1000 ps, with nonbonded interaction cutoffs at 110.0 Å. Configurations were saved every picosecond, resulting in a total of 1000 conformations for each ligand. This procedure is similar to the procedure adopted by Beech et al.⁶⁰ in generating conformers of 1,4,7-trithiacyclononane. That study included a comparison of results obtained from the approach adopted here against grid-based and Monte Carlo-based search algorithms. All three approaches agreed on the 13 lowest conformations.

The 1000 thiacycrown geometries were optimized at 0 K using CVFF/MM and the Broyden–Fletcher–Goldfarb–Shanno (BFGS)⁶¹ optimization algorithm. The resulting conformer energies were energy sorted and duplicate conformations were eliminated. The lowest energy structure predicted by molecular mechanics was subjected to further MD simulations (at 1000 and 500 K). This limited simulated annealing produced no new low-lying conformations for 9t3 and 12t4, but did uncover additional conformers for the larger rings.

Approximately 20 of the lowest energy MM conformers were then reoptimized at the RHF/3-21G level.⁶² The MM energy range spanned by these configurations was \sim 4 kcal/mol, in keeping with our goal of identifying conformations within several kcal/mol of the global minimum. Experience indicated that CVFF tends to underestimate the conformational energy difference predicted by higher levels of theory. RHF/3-21G optimization resulted, in general, in a revised energy ordering. Next, RHF/3-21G structures were used as initial guesses for RHF/6-31+G* geometry optimizations and frozen core (FC) MP2 energy evaluations. A few of the structures were reoptimized at the MP2 level of theory with the correlation consistent aug-cc-pVDZ basis set (denoted aVDZ).^{63,64}

Normal-mode analyses were performed for the lowest ten RHF/3-21G and lowest six RHF/6-31+G* conformations of each thiacycrown, in order to ensure that the structures represented a true minima. Occasionally other structures were considered that were not harvested from the MD/MM simulations, but were based on chemical intuition. All RHF structures were optimized using Gaussian's "tight" criterion, corresponding to a maximum force on the atoms of 1.5×10^{-5} hartree/bohr. Some of the MP2/aVDZ calculations were run with NWChem⁶⁵ on the 512-node SP2 in the Molecular Science Computing Facility.

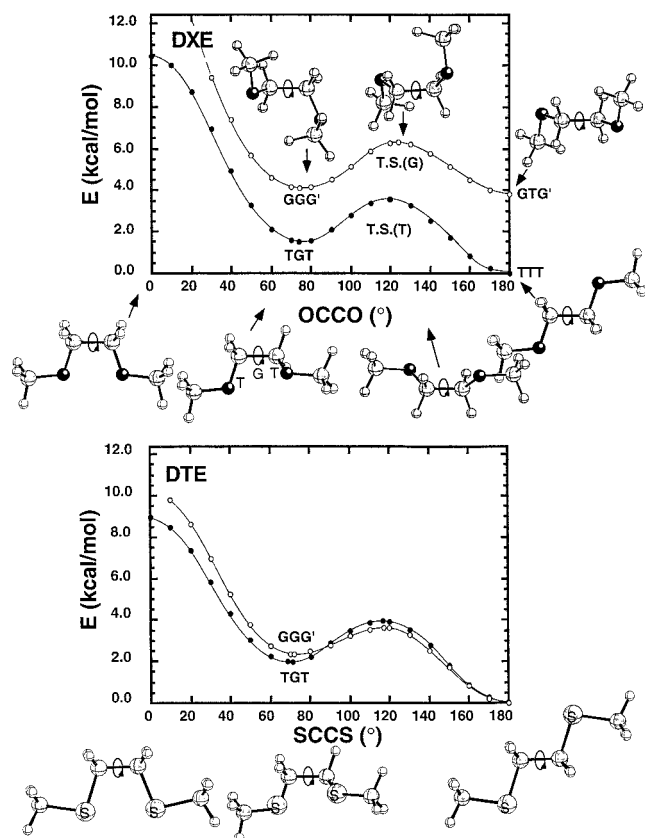


Figure 1. RHF/6-31+G* potential energy curves for rotation about the central C–C bond in dimethoxyethane (DXE) and dithiomethylethane (DTE). The curve with the solid circles corresponds to trans COCC and CCOC angles (or trans CSCC and CCSC angles for DTE). The open circles correspond to gauche COCC and CCOC angles of approximately $\pm 80^\circ$.

III. Results and Discussion

A. 1,2-Dimethoxyethane and 1,2-Dithiomethylethane. Previous studies^{31,66–74} of 1,2-dimethoxyethane (DXE) in liquid and gas phases have identified two low-lying minima. As shown in the top portion of Figure 1, the trans–gauche–trans (TGT) and all-trans (TTT) conformations from the lower energy surface differ primarily by a simple torsional rotation about the central C–C bonds. Although RHF/6-31+G* theory predicts that the TTT conformation is ~ 2 kcal/mol lower in energy than TGT, more extensive calculations have shown that this energy difference tends toward zero as the sophistication of the quantum mechanical treatment increases.^{31,71,72} Metal cations bind to the TGT conformation.

DXE and its sulfur analogue, 1,2-dithiomethylethane (DTE), contain a total of five bonds about which rotation could occur. However, we focus our discussion on the role played by the central dihedral bond, since rotations of the terminal methyl groups have no counterpart in the thiocrowns. The two potential energy curves shown in each half of Figure 1 represent typical configurations of the $-\text{COC}_2\text{H}_4\text{OC}-$ and $-\text{CSC}_2\text{H}_4\text{SC}-$ subunits of the oxygen- and sulfur-bearing crowns. With the exception of the central dihedral angle, all other geometric parameters were optimized.

Both DXE curves contain two minima and two transition states. The smaller barrier near 120° is of the same order of magnitude as the rotational barrier in ethane. The higher barrier ($\text{OCCO} = 0^\circ$) results from (1) the oxygen–oxygen repulsion in the case of the TxT curve and (2) sharply increased steric

repulsion as the two terminal methyl groups contact each other in the GxG' curve. The TxT curve for DXE generally lies 2–4 kcal/mol lower in energy than the GxG' curve because of the increased steric repulsion in the latter. TxT conformations also possess smaller dipole moments than the GxG' conformations, e.g. $\mu(\text{TGT}) = 1.8$ D vs $\mu(\text{GGG}') = 2.4$ D. The increase in the C–S bond lengths in DTE, compared to the C–O bonds in DXE, is responsible for the nearly superimposed potential curves in the lower portion of Figure 1. The dipole moments for the TGT and GGG' configurations are both ~ 2.8 D. In general, conformers with the smallest dipole moment have the lowest energy.

A comparison of RHF/6-31+G* relative conformer energies calculated at RHF optimized geometries [RHF(RHF)] and MP2 results at either the RHF geometries [MP2(RHF)] or at MP2-optimized geometries [MP2(MP2)] showed variations of ± 2 kcal/mol. While such effects are small in an absolute sense, their size will increase with system size. MP2 reduces the TTT–GTG' split in DXE from 3.8 to 3.1 kcal/mol. As already mentioned, the TGT–TTT split falls from around 2 kcal/mol (RHF/6-31+G*) to near zero with large basis sets and the MP2 level of theory. For DTE, MP2 increases the TTT–GTG' split from near zero to 1.1 kcal/mol, with GTG' lower in energy. In summary, the preferred gas phase conformations are predicted to be TTT (DXE) and GTG' (DTE). These findings are in accord with the Raman and infrared spectral data of Ogawa and co-workers.⁷⁵ Furthermore, these conformations are also found in the crystalline liquid states.

B. 9-Thiacrown-3. The smallest of the thiocrown ethers examined in this work is 9-thiacrown-3 (9t3). As evidenced by the number of $\text{M}^+/\text{9t3}$ complexes and $\text{9t3}/\text{M}^+/\text{9t3}$ sandwich complexes referenced in the Cambridge database, this molecule favors a conformation with C_3 symmetry when bonded to an ion,⁷⁶ since it enables the molecule to effectively bind metal cations by placing all three sulfur atoms on the same side of the macrocycle (see Figure 2). The gas phase conformation is less well characterized. A gas phase structure was reported by Blom et al.³⁹ using a combination of gas phase electron diffraction data and molecular mechanics calculations. Of the four symmetries considered (D_3 , C_3 , C_2 , and C_1), the C_1 structure provided the best fit to the experimental data, followed closely by the C_2 conformation. Blom et al. were unable to rule out the possibility of small amounts of a C_3 conformation being present in their gaseous samples at 500 K. A more comprehensive theoretical search was carried out by Beech and co-workers⁶⁰ using MD and Monte Carlo techniques, on both free 9t3 and its metal complexes. Comparison with our results will be made below.

A comparison of selected mean structural parameters obtained from the crystal structure⁷⁶ and from geometry optimizations at the RHF/6-31+G* and MP2/aVDZ levels of theory of the C_3 conformation are presented in Table 1. The observed differences in bond lengths (± 0.01 – 0.02 Å) are typical of other carbon/silicon compounds.⁷⁷

The 1000 MD conformations, generated via the 2000 K procedure described above, contained 38 unique structures within 14 kcal/mol of the MM global minimum. MD calculations run at 500 K produced only one conformation within 15 kcal/mol of the global minimum. The sensitivity of the results to temperature is indicative of a relatively high barrier to reorientation and is a consequence of the small size of the macrocycle. Similar behavior was not observed with the larger rings. The distribution of conformer energies is shown in Figure 2 at four levels of theory: MM, RHF/3-21G, MP2(RHF)/6-

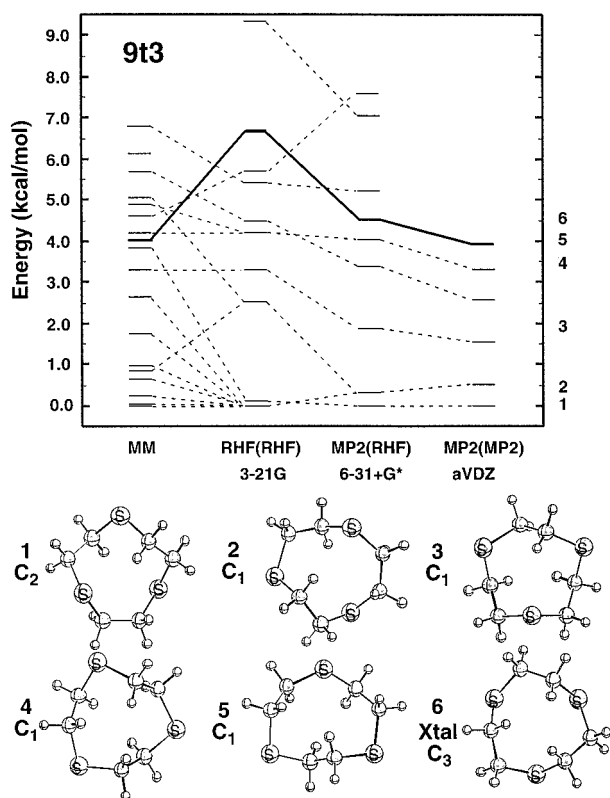


Figure 2. Relative electronic energies of 9t3 conformations. The solid thick line traces the energy of the crystal structure. The notation MP2-(RHF) means that the MP2 energy was evaluated at the optimal RHF geometry. The aVDZ energies were evaluated at the optimal MP2/aVDZ geometries.

31+G*, and MP2(MP2)/aVDZ. A dotted line is used to connect structures with equivalent dihedral angle sequences around the macrocycle and the solid line traces the energy of the crystal structure.

It is evident in Figure 2 that many of the MM conformations collapse to the same RHF/3-21G structure. This is particularly

true of the lowest RHF energy conformation. In addition, there are substantial changes in energy order among the MM, RHF/3-21G, and MP2/6-31+G* results. By comparison, increasing the level of theory to MP2/aVDZ results in relatively minor changes, suggesting that the MP2(RHF)/6-31+G* theory are within a kcal/mol or so of the converged results.

Relative energies and dipole moments for the eight lowest energy structures are presented in Table 2, where they are compared with results taken from the literature. The two previous MM studies predicted the crystal structure (6) to be among the lowest energy conformations, whereas our ab initio results show it to be ~5 kcal/mol above the C₂ minimum. The dipole moment values loosely track the conformer's relative energy, with the crystal structure displaying the largest value ($\mu = 4.5$ D). The two lowest ab initio conformers are the same structures that produced the best fit to the gas phase electron diffraction data of Blom et al.³⁹ Zero-point vibrational corrections shift relative energies by up to 0.3 kcal/mol across an energy span of 7 kcal/mol (conformers 1–7), but the effect on close-lying conformers is less.

Conformers are identified by the sequence of dihedral angles, whose values are given for all of the thiocrowns in Table 3. An MP2 optimization of the C₂ structure showed an overall size contraction, with bond lengths shrinking by ≤ 0.004 Å, bond angles decreasing by $\leq 2^\circ$, and dihedrals differing by $\leq 1^\circ$. S...S distances decreased by as much as 0.038 Å.

C. 12-Thiocrown-4. Among the thiocrowns examined here, 12t4 exhibits the most pronounced exodentate profile. Its even-membered ring permits the dihedral angle sequence to remain in phase, resulting in a high-symmetry (D_4), nearly planar structure (see Figure 3). D_4 is also the symmetry of the crystal structure.³⁷ The 1000 MD conformations contained 168 unique structures with energies ≤ 16 kcal/mol when run at 2000 K. At 1000 K there were 130 unique energies, and at 500 K there were 68. Thus, 12t4 appears much less sensitive to the temperature of the simulation, suggesting lower barriers to interconversion among the conformers. All levels of theory agree on the global minimum.

TABLE 1: Mean Theoretical and Experimental Structural Parameters

system		S–C (Å)	C–C (Å)	S...S _{max} (Å)	C–S–C (deg)	S–C–C (deg)	S–C–C–S (deg)	C–S–C–C (deg)		
9t3	RHF/6-31+G*	1.820	1.533	3.525	103.4	116.7	56.8	56.1	–128.4	
	MP2/aVDZ	1.832	1.535	3.443	100.9	116.5	55.8	58.4	–132.0	
	expt ^a	1.822	1.510	3.454	102.8	115.1	58.6	55.1	–131.1	
12t4	RHF/6-31+G*	1.822	1.529	6.341	102.3	114.0	187.7	72.0		
	MP2/aVDZ	1.836	1.528	6.344	99.9	112.7	175.7	72.3		
	expt ^b	1.814	1.512	6.354	101.3	113.8	186.6	72.2		
15t5	RHF/6-31+G*	1.822	1.528	7.444	102.0	113.7	–67.9	177.6	–86.6	111.3
	expt ^b	1.836	1.478	7.289	101.6	111.8	–63.9	174.0	–89.1	115.1
18t6	RHF/6-31+G*	1.824	1.527	8.933	103.3	114.3	67.9	182.0	94.4	–84.1
	expt ^c	1.854	1.432	8.988	102.2	112.1	75.3	183.0	93.3	–85.6

^a CSD label = THCYNE, ref 76. ^b CSD label = FOPCAO (12t4) and FOPCES (15t5), ref 37. ^c CSD label = BOWROU, ref 36.

TABLE 2: Symmetries, Dipole Moments, and Relative Conformational Energies of 9-Thiocrown-3

conformer	sym	μ (D) ^a	MM/CVFF	RHF(RHF) 3-21G	relative energy (kcal/mol)			Blom et al. ^b	Beech et al. ^c
					MP2(RHF) 6-31+G*	MP2(MP2) aVDZ			
1	C ₂	1.7	0.0	0.1	0.0 ^d	0.0 ^e	1.98	0.60 (g)	
2	C ₁	1.7	0.0	0.0	0.3	0.6	0.00	0.31 (b)	
3	C ₁	2.9	3.3	3.3	1.9	1.5		3.00 ^f (f)	
4	C ₁	0.0	4.6	4.5	3.4	2.3		2.78 (j)	
5	C ₁	1.5	4.2	4.2	4.0	3.3		3.60 (h)	
6 (xtal)	C ₃	4.5	4.0	6.6	4.5	3.9	0.03	0.00 (a)	
7	C ₁	2.3	4.3	5.4	5.2			3.99 (k)	
8	C ₁	4.4	5.1	9.4	7.1			3.04 ^l (e)	

^a Dipole moments were obtained at the RHF/6-31+G* level of theory. ^b Reference 39. ^c Reference 60. Labels in parentheses are notation from this reference. ^d $E(\text{MP2}/6-31+G^*) = -1427.87529 E_h$. ^e $E(\text{MP2}/a\text{VDZ}) = -1428.12531 E_h$. ^f Conformer match uncertain.

TABLE 3: RHF/6-31+G* Skeletal Dihedral Angles (deg)

		C-C	C-S	S-C	C-C	C-S	S-C	C-C	C-S	S-C	C-C	C-S	S-C	C-C	C-S	S-C	C-C	C-S	S-C	
9t3	1	-66	-61	105	-85	105	-61	-66	71	71										
	2	-92	130	-89	76	-114	72	63	-116	68										
	3	119	-54	-76	62	75	71	-56	101	-86										
	4	-135	80	-88	132	-88	80	-135	68	68										
	5	99	-58	94	-162	64	49	-111	107	-117										
	6	57	-128	56	57	-128	56	57	-128	56										
12t4	1	-172	72	72	-172	72	72	-172	72	72	-172	72	72							
	2	171	-97	82	-170	80	77	-166	77	80	-170	82	-97							
	3	168	-83	-83	168	-92	91	-168	83	83	-168	92	-91							
	4	84	-154	80	82	-74	-64	179	-75	-92	72	87	-120							
	5	169	-76	-90	76	92	-92	-76	90	76	-169	87	-87							
	6	174	-113	69	-95	-179	-85	-73	104	-102	-169	-75	-80							
15t5	1	-173	-73	-77	179	174	99	-72	99	174	170	-77	-73	-173	-66	-66				
	2	177	-86	-80	-174	-80	-77	-168	-80	-87	-172	-104	67	172	159	-86				
	3	179	167	-88	169	-90	-88	174	-90	177	172	69	-99	-180	-146	76				
	4	-179	68	-103	176	169	102	-72	105	175	176	-77	-77	169	-79	167				
	5	-175	-73	-79	176	174	98	-83	122	-84	-174	172	-77	170	-70	-66				
	6	170	-81	171	179	74	-124	-176	-84	-89	179	-85	154	-179	74	-142				
	7	178	168	-80	166	169	91	-76	108	175	-179	-80	-75	-177	-98	70				
	8	177	-175	-90	78	-172	174	-73	96	-166	-178	-76	-77	-173	-103	74				
18t6	9	-178	-82	-90	174	-87	163	176	95	-72	-68	145	73	178	80	-102				
	1	179	-79	-180	180	79	-173	-180	-756	-78	179	-80	-180	180	79	-173	-180	-76	-78	
	2	177	123	-96	68	101	-72	-173	79	76	177	123	-96	68	101	-72	-173	79	76	
	3	178	65	62	173	67	166	172	75	-175	-178	-65	-62	-173	-67	-166	-172	-75	175	
	4	-178	78	-175	178	-78	175	-178	78	-175	178	-78	175	-178	78	-175	178	-78	175	
	5	179	72	-104	-178	-74	-169	-178	-75	-178	179	72	-104	-178	-74	-169	-178	-75	-178	
	6	-176	-71	-165	-176	-75	177	-179	97	-79	180	168	68	175	161	72	175	89	-88	
	7	-179	64	61	174	69	168	169	86	-86	-169	-168	-69	-174	-61	-64	179	-168	168	
	8	176	175	-99	67	78	-165	-177	-152	-69	180	-102	71	177	178	-80	178	174	74	
	9	-170	170	-164	178	-97	76	177	-173	-76	-179	179	77	179	173	-78	175	-160	79	
	10	179	-69	-151	-174	-167	110	-78	104	-176	180	-69	-157	-175	-69	180	-179	71	-102	
	11	178	-168	93	-79	162	179	176	-78	-74	178	-169	93	-79	162	179	176	-78	-74	
12	176	118	-95	70	105	-70	-172	107	-67	-176	-118	95	-70	-105	70	172	-107	67		

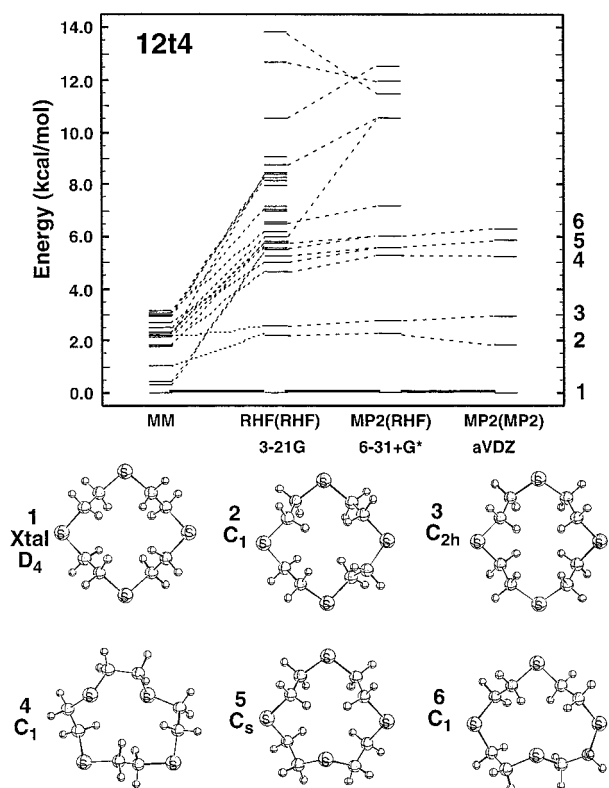


Figure 3. Relative electronic energies of 12t4 conformations. The solid line traces the energy of the crystal structure. The aVDZ energies were evaluated at the optimal MP2/aVDZ geometries.

Compared to 9t3, the MM spectrum of conformational energies is much denser, while the ab initio MP2 spectrum is roughly comparable. Overall, small basis set RHF calculations

predict a wider spread in energies than does molecular mechanics. Although the amount of data is limited, it would appear that this tendency for MM to underestimate the energy differences between conformers would be confirmed by even higher levels of theory. Structures **2** and **3** are out-of-plane distortions of the D_4 conformation. Structure **4** is the first conformation that includes an endodentate torsional angle. Table 4 lists the relative energies. A comparison is made with the corresponding conformations of 12-crown-4 (12c4), for which structures **7–10** represent four of the lowest six conformations.²⁰ C_4 is the symmetry adopted by 12c4 when forming complexes with metal cations and C_i is the crystal structure.⁷⁸ Clearly, these endodentate structures are very high in energy for the sulfur-based crown, just as the D_4 conformation is high in energy for oxygen-bearing crowns. The difference in global minimum geometries between 12c4 and 12t4 is due to the favorable combination of 4-trans/8-gauche dihedral angles about the macrocycle for 12t4, versus a less than ideal 4-gauche/4-trans/4-gauche combination about the C–C/C–O/O–C sequence for 12c4. A ring structure favors a gauche majority, which is sterically costly for the smaller oxygen-based crown. The S_4 conformation of 12c4 is partly stabilized by 1,5 H···O interactions. The sequences of optimal dihedral angles for the lowest lying 12t4 conformations are given in Table 3.

D. 15-Thiacrown-5. The spectrum of 15t5 low-lying conformers (see Figure 4) is dominated by low-symmetry structures. An extensive conformational search of the oxygen-bearing ether analogue (15-crown-5), performed by Paulsen et al.⁷⁹ with the MM3 force field, also reported a predominance of low-symmetry species among the lowest energy conformations. The number of unique MM 15t5 structures with energies below 18 kcal/mol increased sharply compared to the smaller crowns. The MD simulations at 2000 K produced 666 unique structures. The

TABLE 4: Symmetries, Dipole Moments, and Relative Conformational Energies of 12-Thiacycrown-4 and 12-Crown-4

conformer	sym	μ (D)	MM/CVFF	relative energy (kcal/mol)			12-crown-4 ^a
				RHF(RHF) 3-21G	MP2(RHF) 6-31+G*	MP2(MP2) aVDZ	
1 (xtal)	D_4	0.0	0.0	0.0	0.0 ^b	0.0 ^c	23.7
2	C_1	0.2	1.0	2.2	2.3	1.8	
3	C_{2h}	0.0	2.2	2.6	2.7	2.9	
4	C_1	3.7	1.8	4.7	5.3	5.3	
5	C_s	3.5		5.3	5.6	5.8	
6	C_1	3.4	2.2	5.6	6.0		
7	C_i	0.0		6.6	7.2		2.5
8	S_4	0.0		8.7	10.5		0.0
9	C_4	6.2		13.8	11.4		8.3
10	C_s	3.7		12.7	11.9		4.6

^a Reference 29. Relative energies of 12-crown-4 are quoted at the MP2/6-31+G* level. ^b $E(\text{MP2}/6\text{-}31\text{+}G^*) = -1903.8513 E_h$. ^c $E(\text{MP2}/\text{aVDZ}) = -1904.1875 E_h$.

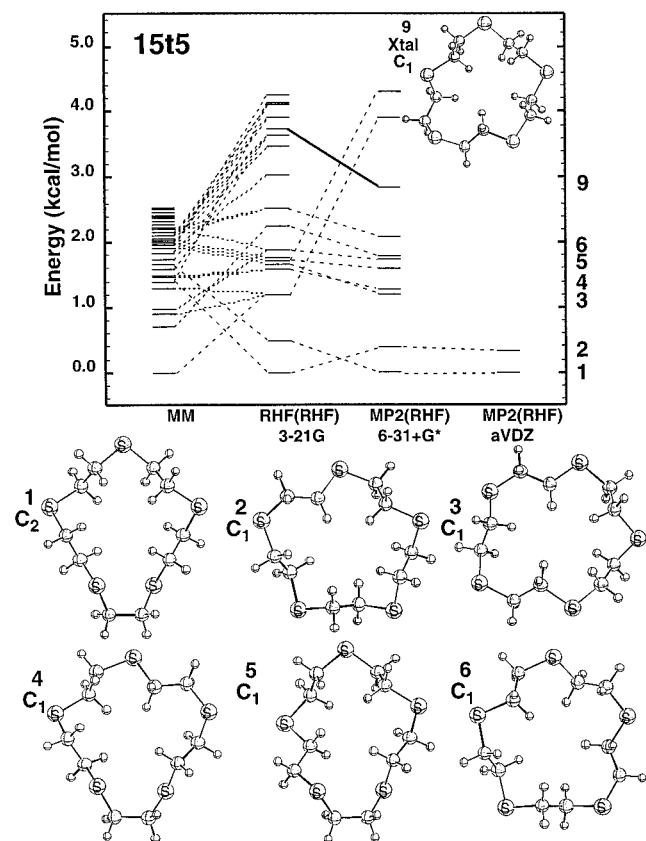


Figure 4. Relative electronic energies of 15t5 conformations. The solid line traces the energy of the crystal structure.

crystal structure sits about 3 kcal/mol above the lowest energy conformation, with 8 lower-lying structures identified at the MP2 level.

The lowest-lying conformations fall into two general categories: those with five trans SCCS dihedrals, possessing a roughly circular shape ($\mu \sim 0.5$ D), and those with four trans and one gauche SCCS dihedral giving an oblong shape ($\mu \sim 2$ D). The latter characterizes the lowest energy conformer found here (**1**), which is of C_2 symmetry.

Relative energies for 15t5 are listed in Table 5, where the crystal structure³⁷ is labeled **9**. MM structures below 2.2 kcal/mol were utilized for the quantum mechanical analysis, resulting in 28 unique RHF/3-21G configurations and 18 RHF(RHF)/6-31+G* configurations. MP2 calculations were performed on the lowest nine of these. MP2/6-31+G* geometry optimization of **1** resulted in an overall size contraction, similar to what was observed for the smaller thiacycrowns. Bond lengths shortened by ~ 0.004 Å, and bond angles were reduced by $\sim 2^\circ$. The cross-

TABLE 5: Symmetries, Dipole Moments, and Relative Conformational Energies of Theoretical Conformations of 15-Thiacycrown-5

conformer	sym	μ (D)	MM/CVFF	relative energy (kcal/mol)		
				RHF(RHF) 3-21G	MP2(RHF) 6-31+G*	MP2(RHF) aVDZ
1	C_2	2.5	1.5	0.0	0.0	0.00 ^a
2	C_1	0.5	1.7	0.5	0.4	0.4
3	C_1	0.5	2.0	1.7	1.2	
4	C_1	2.1	1.5	1.6	1.3	
5	C_1	2.2	2.0	1.8	1.6	
6	C_1	0.3	1.0	1.9	1.7	
7	C_1	2.3	0.7	2.3	1.8	
8	C_1	4.1	2.2	2.5	2.1	
9 (xtal)	C_1	2.0		3.7	2.8	

^a $E(\text{MP2}/\text{aVDZ}) = -2380.2306 E_h$.

ring S...S distances decreased by up to 0.242 Å and several dihedrals changed by as much as $\pm 6^\circ$.

E. 18-Thiacycrown-6. Comparison between the RHF/6-31+G* structure of 18t6 and the X-ray data^{36,37} (Table 1) shows relatively good agreement. MP2 calculations predict the crystal structure to lie within 1 kcal/mol of the lowest energy gas phase structure (see Figure 5), although RHF calculations predict it to be as much as 6 kcal/mol higher. As expected, the conformational energy spectrum of 18t6 is characterized by the highest density of the four thiacycrowns examined here. Over 1000 unique MM configurations, many possessing high symmetry, were identified with energies below 18 kcal/mol. Obviously, for a system as large as 18t6, an exhaustive search of the conformational space is a nontrivial task.

With the exception of the crystal structure (labeled **2** in Figure 5), the six lowest energy conformations have fully exodentate structures (i.e., all trans SCCS and mainly gauche CSCC dihedral angles) in common. The heavy atoms in these conformations form a shallow bowl. Relative energies are given in Table 6. RHF and MP2 relative energies generally agree to within ± 2 kcal/mol. Two exceptions are the crystal structure (**2**) and structure **12**, a C_i symmetry analogue of **2**. Both of these structures are folded, with two endodentate and four exodentate donors. Each is substantially stabilized at the MP2 level, relative to the other conformations. This effect is especially pronounced with the 6-31+G basis set, since RHF/6-31+G* calculations increase the energy gap between the global minimum and structures **2** and **12** by ~ 3 kcal/mol, relative to RHF/3-21G.

Structures **1**, **2**, and **12** are compared with the C_i crystal structure⁸⁰ of 18c6 in Figure 6. In 18c6, the C_i gas phase global minimum can be rationalized in terms of a pair of attractive 1,5 H...O interactions. By adopting exodentate oxygen orientations in the 1,5 positions, the C_i conformer lies ~ 5 kcal/mol

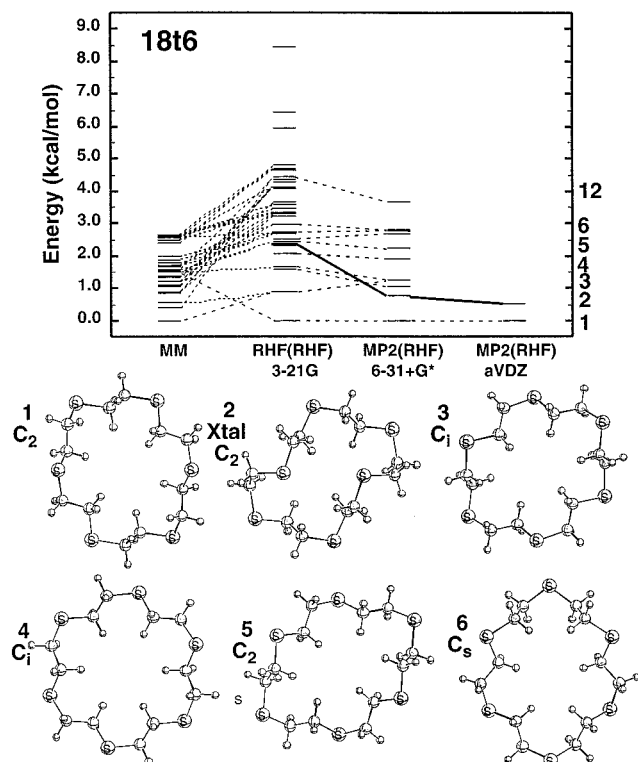


Figure 5. Relative electronic energies of 18t6 conformations. The solid line traces the energy of the crystal structure

TABLE 6: Symmetries, Dipole Moments, and Relative Energies of Theoretical Conformations of 18-Thiacrown-6

conformer	sym	μ (D)	MM/CVFF	relative energy (kcal/mol)	
				RHF(RHF) 3-21G	MP2(RHF) 6-31+G*
1	C_2	0.1	1.4	0.0	0.0
2	C_2	0.9	0.0	2.3	0.8
3	C_i	0.0	2.3	1.6	1.1
4	C_i	0.0	0.6	0.9	1.3
5	C_2	0.1	1.5	1.7	1.3
6	$\sim C_s$	0.2		2.1	1.8
7	C_s	0.3		2.5	1.9
8	C_1	2.2	2.6	2.7	2.3
9	C_1	0.4	1.5	2.5	2.7
10	C_1	2.2	1.5	3.0	2.8
11	C_2	0.5	1.7	2.7	2.8
12	C_i	0.0		4.3	3.7

lower than the fully endodentate D_{3d} conformation.⁵⁸ Although 18t6 prefers the fully exodentate C_2 conformation, structures **2** and **12** can partially offset the cost of two endodentate sulfurs with stabilizing trans-annular $H\cdots S$ interactions. The distances involved in these interactions are 3.297, 3.212, 3.848, and 3.535 Å, respectively.

To estimate the correlation energy contributions to these attractive interactions, an $H\cdots S$ interaction potential was computed using the dimethyl sulfide (CH_3SCH_3) dimer as a model for the thiocrown moieties. After correcting for the undesirable effects of basis set superposition error (BSSE) via the counterpoise method,⁸¹ the dimethyl sulfide dimer binding curve showed an MP2 correlation correction of ~ 0.7 kcal/mol range per $H\cdots S$ interaction (see Figure 7). The size of the correction increased as the $H-S$ distance decreased. The MP2 BSSE-corrected binding curve displayed a minimum near 3.1 Å, similar to, but slightly shorter than, the $H-S$ distances in **2** and **12**. If we crudely estimate the overall stabilization from these interactions by summing the increases to the binding

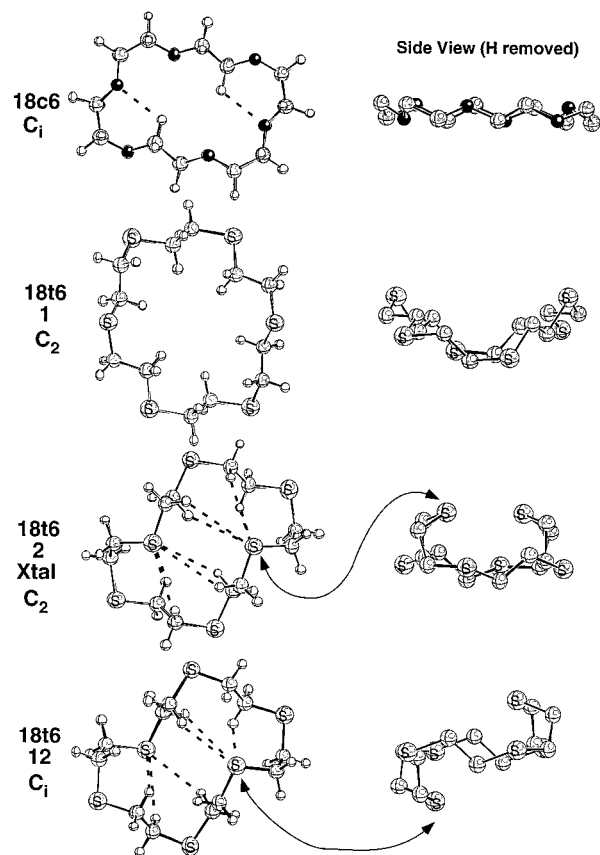


Figure 6. 18-Crown-6, 2-folded structures of 18t6, and the lowest gas phase conformation of 18t6. Side views are shown with hydrogens absent.

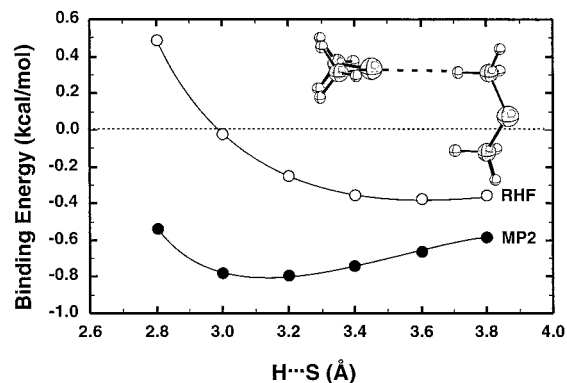


Figure 7. $H\cdots S$ potential energy curves for the dimethyl sulfide dimer at the counterpoise-corrected RHF and MP2 levels with the 6-31+G* basis set.

energy in our model dimer system, we obtain 4–6 kcal/mol, which can be compared with the RHF \rightarrow MP2 18t6 stabilizations of 5.3 and 4.8 kcal/mol, respectively, for **2** and **12**. While we corrected for BSSE in our model system, it is difficult to define such a correction for relative conformational energies in a molecule like 18t6.

IV. Summary

A conformational analysis of four thiocrown ethers was performed using a combination of classical molecular dynamics and correlated ab initio methods. In some cases the gas phase global minimum was as much as 5 kcal/mol lower in energy than the crystal structure. The results were not found to be sensitive to the level of basis set, as long as a set of valence

double- ζ quality or better was used. In the worst cases, MP2 changed the RHF energy orderings by as much as 3 kcal/mol.

Computed torsional barriers for acyclic DTE suggest a strong preference for trans SCCS dihedrals and a weaker preference for gauche CSCC dihedrals. At least two-thirds of the CSCC angles in the thiacyclics were gauche and the lowest energy structures for each ring size were 80–100% gauche CSCC. While the preferred dihedral angle sequences play a dominant role, the size of each thiacyclic imposes additional boundary conditions that result in unique features for each ring size. All of the thiacyclics tended to adopt exodentate structures. Examples of folded structures were not produced in the MD simulation for any of the thiacyclics, although several low-lying folded structures were found for 18t6 (e.g., **2** and **12**), including the crystal structure. Given the failure of the MD procedure to generate folded structures, it is impossible to rule out the existence of additional cases for 18t6.

Acknowledgment. The authors thank Dr. Edgar Arcia for a careful reading of the manuscript prior to publication. This research was supported by the U.S. Department of Energy under contract no. DE-AC06-76RLO 1830. The authors also acknowledge the support of the Division of Chemical Sciences, Office of Basic Energy Sciences. S.E.H. acknowledges the support of the Associated Western Universities, Inc. (on behalf of Washington State University) under grant no. DE-FG06-89ER-75522 with the U.S. Department of Energy. The authors are grateful to Dr. Mark A. Thompson for providing substantial assistance with the MD/MM simulations. Portions of this work were completed on the computer resources at the National Energy Research Supercomputer Center with a grant provided by the Scientific Computing Staff, Office of Energy Research, U.S. Department of Energy. The Pacific Northwest National Laboratory is a multiprogram national laboratory operated by Battelle Memorial Institute.

References and Notes

- (1) Billeter, M.; Howard, A. E.; Kuntz, I. D.; Kollman, P. A. *J. Am. Chem. Soc.* **1988**, *110*, 8385–8391.
- (2) Fukuhara, K.; Ikeda, K.; Matsuura, H. *J. Mol. Struct. (THEOCHEM)* **1990**, *224*, 203–224.
- (3) von Szentpály, L. S.; Shamovsky, I. L. *J. Mol. Struct. (THEOCHEM)* **1994**, *305*, 249–260.
- (4) Ranghino, G.; Romano, S.; Lehn, J. M.; Wipff, G. *J. Am. Chem. Soc.* **1985**, *107*, 7873–7877.
- (5) Straatsma, T. P.; McCammon, J. A. *J. Chem. Phys.* **1989**, *91*, 3631–3637.
- (6) Ha, Y. L.; Chakraborty, A. K. *J. Phys. Chem.* **1993**, *97*, 11291–11299.
- (7) Kowall, T.; Geiger, A. *J. Phys. Chem.* **1994**, *98*, 6216–6224.
- (8) Fukuhara, K.; Tachikake, M.; Matsumoto, S.; Matsuura, H. *J. Phys. Chem.* **1995**, *99*, 8617–8623.
- (9) Yamabe, T.; Hori, K.; Akagi, K.; Fukui, K. *Tetrahedron* **1979**, *35*, 1065–1072.
- (10) Wipff, G.; Weiner, P.; Kollman, P. *J. Am. Chem. Soc.* **1982**, *104*, 3249–3258.
- (11) Hori, K.; Yamada, H.; Yamabe, T. *Tetrahedron* **1983**, *39*, 67–73.
- (12) Drew, M. G. B.; Nicholson, D. G. *J. Chem. Soc., Dalton Trans.* **1986**, 1543–1549.
- (13) Burns, J. H.; Kessler, R. M. *Inorg. Chem.* **1987**, *26*, 1370–1375.
- (14) Hase, W. L.; Richou, M.-C.; Mondro, S. L. *J. Phys. Chem.* **1989**, *93*, 539–545.
- (15) von Szentpály, L. S.; Shamovsky, I. L.; Nefedova, V. V.; Zubkus, V. E. *J. Mol. Struct. (THEOCHEM)* **1994**, *308*, 125–140.
- (16) Hancock, R. D. *J. Inclusion Phenom. Mol. Recognit. Chem.* **1994**, *17*, 63–80.
- (17) Dang, L. X. *J. Am. Chem. Soc.* **1995**, *117*, 6954–6960.
- (18) Dang, L. X.; Kollman, P. A. *J. Phys. Chem.* **1995**, *99*, 55–58.
- (19) Wasada, H.; Tsutsui, Y.; Yamabe, S. *J. Phys. Chem.* **1996**, *100*, 7367–7371.
- (20) Feller, D.; Aprà, E.; Nichols, J. A.; Bernholdt, D. E. *J. Chem. Phys.* **1996**, *105*, 1940–1950.
- (21) Glendening, E. D.; Feller, D. *J. Am. Chem. Soc.* **1996**, *118*, 6052–6059.
- (22) Feller, D. *J. Phys. Chem. A* **1997**, *101*, 2723–2731.
- (23) Hiraoka, M. *Studies in Organic Chemistry 12: Crown Compounds—Their Characteristics and Applications*; Elsevier: Amsterdam, The Netherlands, 1982.
- (24) DeSimone, R. E.; Glick, M. D. *J. Am. Chem. Soc.* **1976**, *98*, 762–767.
- (25) Setzer, W. N.; Tang, Y.; Grant, G. J.; VanDerveer, D. G. *Inorg. Chem.* **1992**, *31*, 1116–1118.
- (26) Dockal, E. R.; Diaddario, L. L.; Glick, M. D.; Rorabacher, D. B. *J. Am. Chem. Soc.* **1977**, *99*, 4530–4532.
- (27) Diaddario, L. L., Jr.; Dockal, E. R.; Glick, M. D.; Ochrymowycz, L. A.; Rorabacher, D. B. *Inorg. Chem.* **1985**, *24*, 356–363.
- (28) Blower, P. J.; Clarkson, J. A.; Rawle, S. C.; Hartman, J. R.; Wolf, R. E., Jr.; Yagbasan, R.; Bott, S. G.; Cooper, S. R. *Inorg. Chem.* **1989**, *28*, 4040–4046.
- (29) Blake, A. J.; Gould, R. O.; Reid, G.; Schröder, M. *J. Chem. Soc., Chem. Commun.* **1990**, 974–976.
- (30) Blake, A. J.; Taylor, A.; Schröder, M. *J. Chem. Soc., Chem. Commun.* **1993**, 1097–1098.
- (31) Ray, D.; Feller, D.; More, M. B.; Glendening, E. D.; Armentrout, P. B. *J. Phys. Chem.* **1996**, *100*, 16116–16125.
- (32) Hill, S. E.; Feller, D. *Int. J. Mass Spectrom.*, in press.
- (33) Glendening, E. D.; Feller, D.; Thompson, M. A. *J. Am. Chem. Soc.* **1994**, *116*, 10657–10669.
- (34) Hay, B. P.; Rustad, J. R. *J. Am. Chem. Soc.* **1994**, *116*, 6316–6326.
- (35) Thompson, M. A., private communication.
- (36) Hartman, J. R.; Wolf, R. E.; Foxman, B. M.; Cooper, S. R. *J. Am. Chem. Soc.* **1983**, *105*, 131–132.
- (37) Wolf, R. E., Jr.; Hartman, J. R.; Storey, J. M. E.; Foxman, B. M.; Cooper, S. R. *J. Am. Chem. Soc.* **1987**, *109*, 4328–4335.
- (38) Rawle, S. C.; Admans, G. A.; Cooper, S. R. *J. Chem. Soc., Dalton Trans.* **1988**, 93–96.
- (39) Blom, R.; Rankin, D. W. H.; Robertson, H. E.; Schröder, M.; Taylor, A. *J. Chem. Soc., Perkin Trans. 2* **1991**, 773–778.
- (40) Raithby, P. R.; Shields, G. P.; Allen, F. H. *Acta Crystallogr.* **1997**, *B53*, 241–251.
- (41) Juaristi, E. *Chapter 18*; John Wiley & Sons: New York, 1991.
- (42) Piela, L.; Olszewski, K. A.; Pillardy, J. *J. Mol. Struct. (THEOCHEM)* **1994**, *308*, 229–239.
- (43) Meza, J. C.; Martinez, M. L. *J. Comput. Chem.* **1994**, *15*, 627–632.
- (44) Saunders: M. *J. Am. Chem. Soc.* **1987**, *109*, 3150–3152.
- (45) Ferguson, D. M.; Raber, D. J. *J. Am. Chem. Soc.* **1989**, *111*, 4371–4378.
- (46) Chang, G.; Guida, W. C.; Still, W. C. *J. Am. Chem. Soc.* **1989**, *111*, 4379–4386.
- (47) Saunders: M.; Houk, K. N.; Wu, Y.-D.; Still, W. C.; Lipton, M.; Chang, G.; Guida, W. C. *J. Am. Chem. Soc.* **1990**, *112*, 1419–1427.
- (48) Böhm, H.-J.; Klebe, G.; Lorentz, T.; Mietzner, T.; Siggel, L. *J. Comput. Chem.* **1990**, *11*, 1021–1028.
- (49) Rocha, W. R.; De Almeida, W. B. *J. Comput. Chem.* **1997**, *18*, 254–259.
- (50) von Szentpály, L.; Shamovsky, I. L.; Ghosh, R.; Dakkouri, M. *J. Phys. Chem. A* **1997**, *101*, 3032.
- (51) Allen, F. H.; Kennard, O. *Chem. Desi. Autom. News* **1993**, *8*, 1, 31–37.
- (52) Hehre, W. J.; Ditchfield, R.; Pople, J. A. *J. Chem. Phys.* **1972**, *56*, 2257–2261.
- (53) Hariharan, P. C.; Pople, J. A. *Theor. Chem. Acta* **1973**, *28*, 213.
- (54) Clark, T.; Chandrasekhar, J.; Spitznagel, G. W.; Schleyer, P. v. R. *J. Comput. Chem.* **1983**, *4*, 294.
- (55) Frisch, M. J.; Trucks, G. W.; Schlegel, H. B.; Gill, P. M. W.; Johnson, B. G.; Robb, M. A.; Cheeseman, J. R.; Keith, T.; Petersson, G. A.; Montgomery, J. A.; Raghavachari, K.; Al-Laham, M. A.; Zakrzewski, V. G.; Ortiz, J. V.; Foresman, J. B.; Cioslowski, J.; Stefanov, B. B.; Nanayakkara, A.; Challacombe, M.; Peng, C. Y.; Ayala, P. Y.; Chen, W.; Wong, M. W.; Andres, J. L.; Replogle, E. S.; Gomperts, R.; Martin, R. L.; Fox, D. J.; Binkley, J. S.; Defrees, D. J.; Baker, J.; Stewart, J. P.; Head-Gordon, M.; Gonzalez, C.; Pople, J. A. *Gaussian 94*, Revision D.1; Gaussian, Inc.: Pittsburgh, PA, 1995.
- (56) Breneman, C. M.; Wiberg, K. B. *J. Comput. Chem.* **1990**, *11*, 361.
- (57) Dauber-Osgurthorpe, P.; Roberts, V. A.; Osgurthorpe, D. J.; Wolff, J.; Genest, M.; Hagler, A. T. *Proteins* **1988**, *4*, 31.
- (58) Thompson, M. A.; Glendening, E. D.; Feller, D. *J. Phys. Chem.* **1994**, *98*, 10465–10476.
- (59) Thompson, M. A.; Schenter, G. K. *J. Phys. Chem.* **1995**, *99*, 6374.
- (60) Beech, J.; Cragg, P. J.; Drew, M. G. B. *J. Chem. Soc., Dalton Trans.* **1994**, 719–729.

- (61) Press, W. H.; Teukolsky, S. A.; Vetterling, W. T.; Flannery, B. P. *Numerical Recipes in C*; Cambridge University Press: Cambridge, UK, 1992.
- (62) Binkley, J. S.; Pople, J. A.; Hehre, W. J. *J. Am. Chem. Soc.* **1980**, *102*, 939–947.
- (63) Dunning, T. H., Jr. *J. Chem. Phys.* **1989**, *90*, 1007–1023.
- (64) Kendall, R. A.; Dunning, T. H., Jr.; Harrison, R. J. *J. Chem. Phys.* **1992**, *96*, 6796–6806.
- (65) Anchell, J.; Apra, E.; Bernholdt, D.; Borowski, P.; Clark, T.; Clerc, D.; Dachsels, H.; Deegan, M.; Dupuis, M.; Dylla, K.; Fann, G.; Fruchtl, H.; Gutowski, M.; Harrison, R.; Hess, A.; Jaffe, J.; Kendall, R.; Kobayashi, R.; Kutteh, R.; Lin, Z.; Littlefield, R.; Long, X.; Meng, B.; Nichols, J.; Nieplocha, J.; Rendall, A.; Stave, M.; Straatsma, T.; Taylor, H.; Thomas, G.; Wolinski, K.; Wong, A. *NWChem, A Computational Chemistry Package for Parallel Computers*, Version 3.3; William R. Wiley Environmental Molecular Sciences Laboratory, Pacific Northwest National Laboratory, P.O. Box 999, Richland, WA 99352-0999, 1997.
- (66) Andersson, M.; Karlström, G. *J. Phys. Chem.* **1985**, *89*, 4957–4962.
- (67) Straatsma, T. P.; McCammon, J. A. *J. Chem. Phys.* **1989**, *90*, 3300–3304.
- (68) Bressanini, D.; Gamba, A.; Morosi, G. *J. Phys. Chem.* **1990**, *94*, 4299–4302.
- (69) Yoshida, H.; Kaneko, I.; Matsuura, H.; Ogawa, Y.; Tasumi, M. *Chem. Phys. Lett.* **1992**, *196*, 601–606.
- (70) Inomata, K.; Abe, A. *J. Phys. Chem.* **1992**, *96*, 7934–7937.
- (71) Murcko, M. A.; DiPaola, R. A. *J. Am. Chem. Soc.* **1992**, *114*, 10010–10018.
- (72) Jaffe, R. L.; Smith, G. D.; Yoon, D. Y. *J. Phys. Chem.* **1993**, *97*, 12745–12751.
- (73) Smith, G. D.; Jaffe, R. L.; Yoon, D. Y. *J. Phys. Chem.* **1993**, *97*, 12752–12759.
- (74) Smith, G. D.; Jaffe, R. L.; Yoon, D. Y. *J. Am. Chem. Soc.* **1995**, *117*, 530.
- (75) Ogawa, Y.; Ohta, M.; Sakakibara, M.; Matsuura, H.; Harada, I.; Shimanouchi, T. *Bull. Chem. Soc. Jpn.* **1977**, *50*, 650–660.
- (76) Glass, R. S.; Wilson, G. S.; Setzer, W. N. *J. Am. Chem. Soc.* **1980**, *102*, 5068–5069.
- (77) Feller, D.; Peterson, K. A. *J. Chem. Phys.* **1998**, *108*, 154.
- (78) Groth, P. *Acta Chem. Scand. A* **1978**, *32*, 279–280.
- (79) Paulsen, M. D.; Rustad, J. R.; Hay, B. P. *J. Mol. Struct. (THEOCHEM)* **1997**, *397*, 1–12.
- (80) Dunitz, J. D.; Dobler, M.; Seiler, P.; Phizackerley, R. P. *Acta Crystallogr.* **1974**, *B30*, 2733–2738.
- (81) Boys, S. F.; Bernardi, F. *Mol. Phys.* **1970**, *19*, 553.